Design of a Disturbance Observer and Model-Based Friction Feedforward to Compensate Quadrant Glitches

Z. Jamaludin, H. Van Brussel and J. Swevers

Abstract Accurate motion control requires measures to compensate the effects of friction that contribute to positioning and contour tracking errors. The complex nonlinear behaviour of friction at motion reversal causes a unique tracking error known as quadrant glitch. Friction can only be partly compensated using linear feedback control strategies such as PID, cascade P/PI or state-feedback control. Model and non-model based friction compensation strategies are necessary to acquire sufficiently high path and tracking accuracy. This paper analyses and validates experimentally three different friction compensation strategies for a linear motor-based xy feed drive of a high-speed milling machine: (i) friction model based feedforward, (ii) an inverse-model-based disturbance observer, and (iii) the combination of friction model feedforward and disturbance observer. Two different friction models are considered: a simple static friction model and the recently developed Generalized Maxwell-slip (GMS) friction model. The combination of feedforward based on the GMS friction model and the inverse model-based disturbance observer yields the smallest radial tracking error and glitches.

1 Introduction

Friction is a highly nonlinear phenomenon especially at velocity reversal. Quadrant glitches, characterized by spikes at quadrant locations during circular motion,

Z. Jamaludin
Department of Mechanical Engineering, Div. P.M.A., Katholieke Universiteit Leuven, Celestijnenlaan 300B, Heverlee, B-3001 Leuven, Belgium; E-mail: zamberi.jamaludin@student. kuleuven.be

H. Van Brussel
Department of Mechanical Engineering, Div. P.M.A., Katholieke Universiteit Leuven, Celestijnenlaan 300B, Heverlee, B-3001 Leuven, Belgium; E-mail: hendrik.vanbrussel@mech.kuleuven.be

J. Swevers
Department of Mechanical Engineering, Div. P.M.A., Katholieke Universiteit Leuven, Celestijnenlaan 300B, Heverlee, B-3001 Leuven, Belgium; E-mail: jan.swevers@mech.kuleuven.be

H. Ulbrich and L. Ginzinger (eds.), Motion and Vibration Control, 143–153.

are a direct result of this highly nonlinear behaviour. Friction can only be partly compensated using linear feedback control strategies such as PID, cascade P/PI or state-feedback control. More advanced technique must be incorporated to achieve sufficiently high path and tracking accuracy.

Several simple and advanced friction models are proposed in the literature. The most simple friction models consider the friction sliding regime only. These models are a static map between friction force and velocity, e.g. viscous, Coulomb and Stribeck friction models. A first attempt in describing the more complex friction behaviour in pre-sliding regime was accomplished in 1977 [4]. In 1995, the LuGre model is proposed. The model captures most of the observed frictional behaviours including Coulomb friction, Stribeck effect, and hysteresis [3]. The model is known for its simplicity and relatively good performance but it fails to describe the hysteresis non-local memory behaviour of friction force in pre-sliding regime.

The Leuven model is an improvement of the LuGre model that includes non-local memory hysteretic behaviour. Recently, a further improvement of the Leuven model, called the Generalized Maxwell-slip (GMS) friction model [1], is developed and exhibits superior results in simulation of friction behaviour in the pre-sliding and sliding regimes. The main disadvantage of the GMS model is its complexity and large number parameters, which complicates its application in control.

Various model and non-model based friction compensation schemes for different applications are discussed in literature. A survey on friction models and compensation methods for control of machines with friction is given in [2]. Several alternative approaches have been developed such as: a Maxwell-slip-model-based nonlinear gain scheduling controller yielding fast response and low steady-state error for friction compensation in electro-mechanical systems [7], a repetitive controller, a non-model based friction compensation approach yielding improve tracking performance and quadrant glitches [8], and the GMS friction model feedforward and a Kalman filter based disturbance observer, yielding the best tracking performance in friction compensation on a dedicated test setup (a tribometer) [6]. This paper focuses on the modelling, identification, and compensation of friction forces in machine tools for accurate drive control system. Both friction-model based feedforward, using a simple static friction model and the advanced GMS model, and an inverse-model disturbance observer [9] are considered.

This paper is organized as follows. Section 2 describes the experimental set-up. Section 3 discusses the different friction models and their identification methods. Section 4 discusses the experimental validation of the different friction compensation schemes and finally, Section 5 concludes the paper.

2 Experimental Set-up

The test setup that is considered in this paper is a linear-drive based xy feed table of a high-speed milling machine (see Figure 1). The upper stage y-axis is driven by a single ETEL iron-core linear motor. The bottom stage x-axis is driven by two ETEL

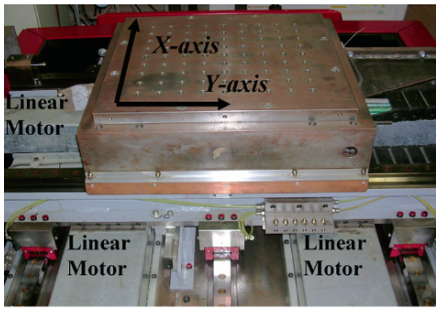

Fig. 1 A xy feed table with three linear drives for high speed milling application.

iron-core linear motors. The stages run on Schneeberger preloaded roller guideways. Both axes are equipped with a 0.25 µm resolution Heidenhain linear encoder. The velocity signal is calculated by means of numerical differentiation of the position in combination with a first-order low-pass filter. This filter is added to attenuate amplified measurement noise associated with the derivative action. The controller is implemented on a dSPACE 1103 DSP controller board linking the host computer to the ETEL drives. The dynamic coupling between both axes is negligible. The system dynamics can be described by two single-input single-output models.

The linear dynamic relation between input voltage and table position z [m], with $z = x$ and $z = y$ for the x and y axes respectively, is identified experimentally as a second order model with a time delay:

$$G(s) = \frac{Z(s)}{U(s)} = \frac{B}{s(s+A)} \cdot e^{-sT_d}, \tag{1}$$

with $A = 28.57$ volt/s, $B = 4.526$ m, $T_d = 0.00065$ s for the x-axis and $A = 20.00$ volt/s, $B = 8.916$ m, $T_d = 0.00065$ s for the y-axis.

3 Friction Models

Friction is categorized according to its presliding and sliding regimes. In pre-sliding regime, friction force is predominantly dependent on displacement. In sliding regime, the friction force is predominantly dependent on the sliding velocity.

3.1 Static Friction Model

Static friction models describe the steady-state friction behaviour in sliding regime and hence are dependent on the sliding velocity v. The considered static friction model incorporates Coulomb, viscous, and Stribeck friction,

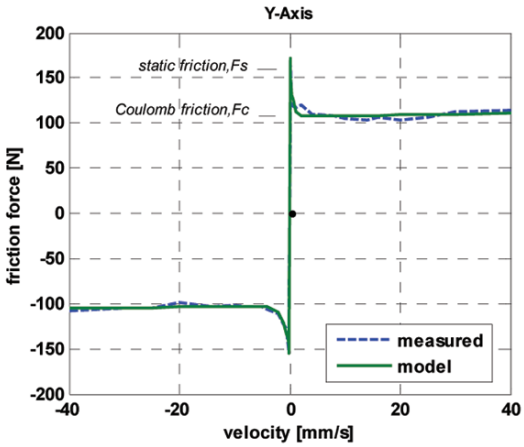

Fig. 2 Measured and modelled static friction-velocity map.

$$F(v) = \left\{ F_c + (F_s - F_c) \cdot \exp\left(- \left| \frac{v}{V_s} \right|^{\delta} \right) + \sigma \cdot |v| \right\} \cdot \text{sign}(v). \tag{2}$$

F_c, F_s, and σ represent the Coulomb, static and viscous friction coefficients respectively. The Stribeck friction model parameters are the Stribeck velocity V_s and the Stribeck shape factor δ.

3.1.1 Identification of Static Friction Model

At constant velocity, the motor force equals the friction force and is represented by the force control command signal. Constant velocity is enforced using a manually tuned PID controller and a constant velocity reference signal. This experiment is repeated for the following constant velocities of 0.010, 0.040, 0.080, 0.2, 0.4, 0.5, 1, 2, 4, 5, 8, 10, 14, 16, 20, 25, and 30 mm/s. Figure 2 shows the measured and the fitted static friction force model (2). The identified parameters are $F_c = 105$N, $F_s = 165$ N, $1/V_s = 0.001$ sμm^{-1}, $\sigma = 0.00004$ Nsμm^{-1}, and $\delta = 1$.

3.2 Generalized Maxwell-Slip Model (GMS) [1]

The GMS friction model incorporates: (i) the Stribeck curve for constant velocity, (ii) hysteresis function with non-local memory for the pre-sliding regime, and (iii) frictional memory for the sliding regime. It has similar structure to the Maxwell-slip structure, that consists of a parallel connection of N different elementary slip-blocks and springs (see Figure 3). Each block represents a generalized asperity of

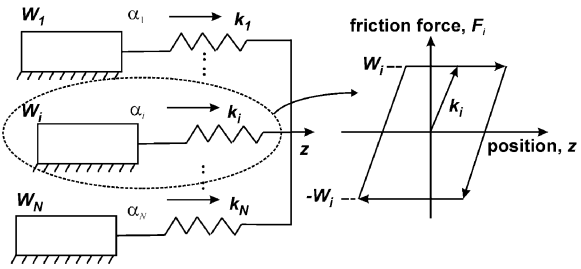

Fig. 3 Maxwell-slip friction with N-elementary slip blocks.

the contact surface that can either stick or slip and each element i has a common input, the position z, an elementary stiffness k_i, a state variable α_i that describes the element position, a maximum elementary Coulomb force W_i and a friction output F_i. A new state equation that characterizes sliding dynamics of each elementary slip-block replaces the original Coulomb law in the Maxwell-slip model structure.

Sticking occurs during motion reversal and as velocity approaches zero. During sticking, the dynamic behaviour of an elementary slip-block is then described by a spring model with stiffness k_i:

$$\frac{\mathrm{d}F_i}{\mathrm{d}t} = k_i v. \tag{3}$$

Slipping occurs if the elementary friction force F_i equals a maximum value $W_i = \alpha_i s(v)$. α_i is the normalized sustainable maximum friction force of each element during sticking and $s(v)$ is the Stribeck curve. The state equation describing the dynamic behaviour of an elementary slip-block is

$$\frac{\mathrm{d}F_i}{\mathrm{d}t} = \operatorname{sign}(v) \cdot C \cdot \left(\alpha_i - \frac{F_i}{s(v)}\right). \tag{4}$$

The constant parameter C indicates the rate at which the friction force follows the Stribeck effect in sliding. The total friction force is the summation of the output of all elementary state models and a viscous friction term σ (if present).

$$F(v) = \sum_{i=1}^{N} F_i(v) + \sigma \cdot v(t). \tag{5}$$

3.2.1 Identification of GMS Model Parameters

A GMS model with four elementary slip-blocks is selected, yielding a total of 13 model parameters: two parameters from each of the four elements and another five parameters from the state equations in sliding regime. Friction behaves as a hysteretic function of displacement with non-local memory behaviour in pre-sliding

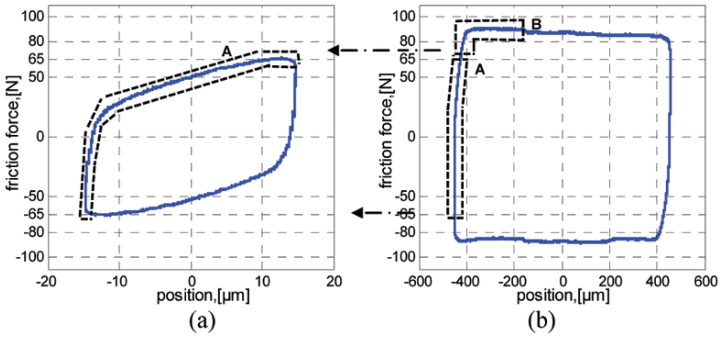

Fig. 4 Friction force and position for sinusoidal reference signal of 0.1 Hz and amplitudes of (a) 15 μm and (b) 450 μm.

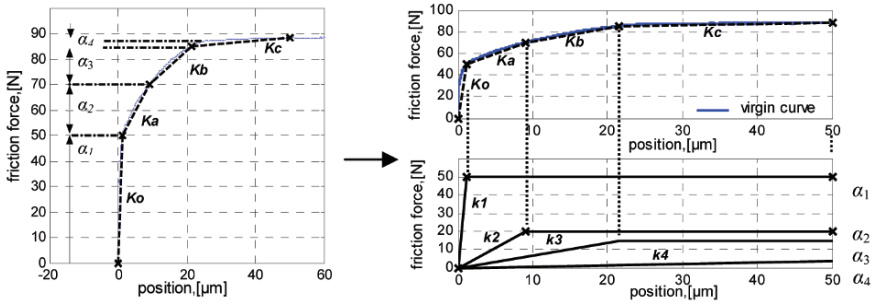

Fig. 5 Virgin curve with selected points for identification of GMS friction model parameters.

Table 1 Identified GMS friction model parameters.

$F_c = 105$ n	$F_s = 165$ N	$V_s = 1000$ μms^{-1}	$\sigma = 0.00004$ Nsμm^{-1}	$\delta = 1$
α_i [N]	$\alpha_1 = 0.566$	$\alpha_2 = 0.227$	$\alpha_3 = 0.170$	$\alpha_4 = 0.039$
k_i [N/μm]	$k_1 = 99.94$	$k_2 = 1.364$	$k_3 = 1.081$	$k_4 = 0.119$

regime. This behaviour is characterized by the so-called virgin curve. The virgin curve is derived from a sinusoidal excitation of the system. The frequency and amplitude of the sinusoidal are selected to minimize inertia effect and to remain in the pre-sliding regime. The measurement obtained with the small excitation amplitude (Figure 4a) provides detailed information about the friction-displacement behaviour in pre-sliding regime away from breakaway, while the measurement obtained with the larger excitation amplitude (Figure 4b) provides information close to breakaway. Figures 4a and b clearly indicate which part of the measurement is selected to compose the virgin curve (see Figure 5). The parts are combined, reduced by a factor of 2 (the combined parts constitute a double-stretched version of the virgin curve), and shifted to the origin (0 μm, 0 N) to generate the virgin curve.

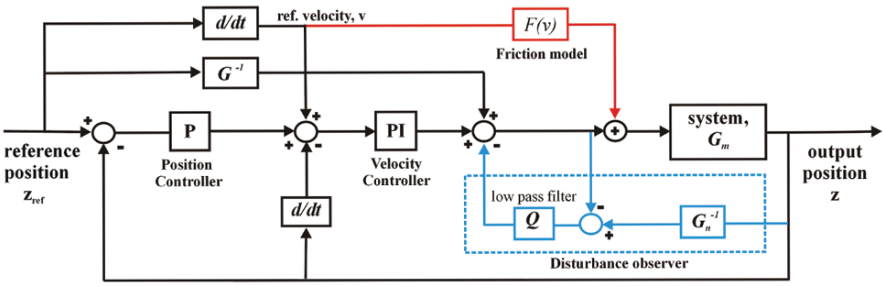

Fig. 6 Cascade P/PI controller with friction model-based feedforward and an inverse-model-based disturbance observer.

The four α_i's and k_i's slip-block parameters are estimated from the manually selected knots and slopes Ko, Ka, Kb, Kc of a piecewise linear function that approximates the virgin curve (see Figure 5). From the theory of superposition, K_i's, k_i's, and α_i's are related as in (6). The identified GMS model parameters and the static friction model parameters (F_c, F_s, V_s, σ, and δ) are summarized in Table 1.

$$\begin{aligned} \alpha_1 + \alpha_2 + \alpha_3 + \alpha_4 &= \Sigma W_i \\ k_1 + k_2 + k_3 + k_4 &= K_o \\ k_2 + k_3 + k_4 &= K_b \\ k_4 &= K_c \ . \end{aligned} \tag{6}$$

4 Friction Force Compensation Design and Experimental Validation

This section discusses the friction compensation design and the experimental validation for the considered system. Each axis is controlled independently using the same control structure shown in Figure 6. It consists of a position controller, static and GMS friction models feedforward, and an inverse-model-based disturbance observer.

4.1 Position Controller and Feedforward Friction Compensation

The position controller is a cascade PI velocity feedback and P position feedback controller. The parameters are selected based on gain margin and phase margin considerations of the open loop transfer function [5]. Velocity feedforward and an inverse-model position reference feedforward are added to eliminate tracking errors

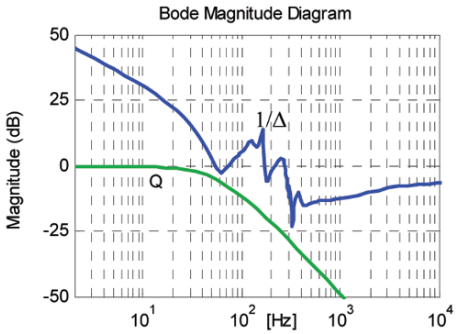

Fig. 7 Bandwidth limitations of the Q-filter.

caused by inertial effects and viscous friction. Feedforward friction compensation is based on either the static friction model (2), or the GMS model (3–5). The input to these models is the reference tracking velocity v.

4.2 Inverse Model-Based Disturbance Observer

The disturbance observer estimates the disturbance forces along with any modelling errors by subtracting the control command signal from the estimated input obtained by the inverse of the nominal plant model $G_n(s)$ which is identical to model (1) without delay. The delay is removed from the plant model in order to obtain a causal inverse. A low pass filter, known as the Q-filter [9], is added to provide system stability. The bandwidth of the filter Q is limited by the unmodelled dynamics, expressed as a multiplicative perturbation $\Delta(f)$,

$$\Delta(f) = \frac{G_m(f) - G_n(f)}{G_n(f)}. \tag{7}$$

$G_m(f)$ and $G_n(f)$ are the frequency response functions of the system and of $G_n(s)$ respectively. The robust stability of the disturbance observer inner loop is guaranteed if [9]

$$||T(j\omega) \cdot \Delta(\omega)||_\infty \leq 1\ . \tag{8}$$

$T(s)$ is the complimentary sensitivity transfer function of the disturbance observer loop. Figure 7 visualizes for the x-axis the Q-filter bandwidth limitation at 60 Hz. The magnitude of the Q-filter frequency characteristic must lie below the amplitude characteristic of the inverse multiplicative perturbation $\Delta(f)$ line and thus limits the observer overall compensation performance.

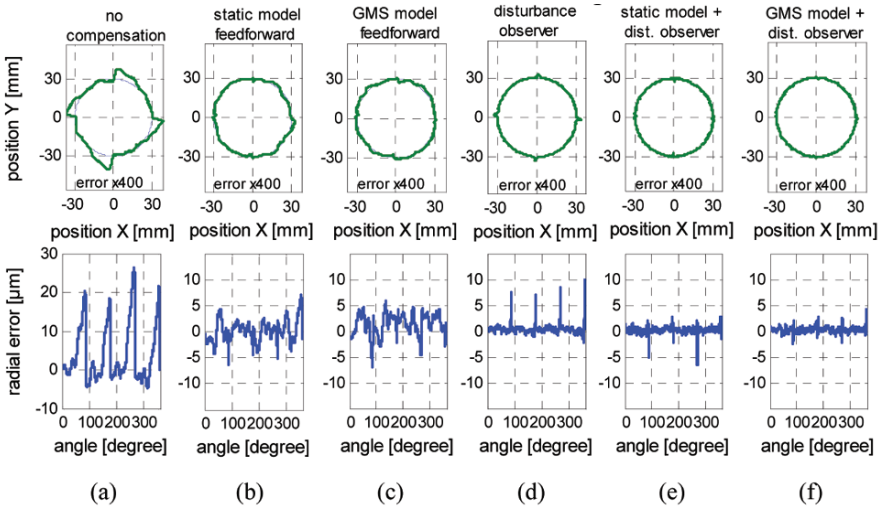

Fig. 8 Measured circular tests (30 mm radius) and radial tracking error for different friction compensation schemes at 100 mm/s tangential tracking velocity.

Table 2 Quadrant glitch magnitudes for different friction compensation strategies.

Friction Compensation Schemes	a	b	c	d	e	f
Quadrant Glitch Magnitude	22 µm	7 µm	6 µm	8 µm	5 µm	3 µm

4.3 Experimental Results

Friction compensation performance is validated based on the magnitude of the quadrant glitch that occurs near zero velocity or at motion reversal. It is typically demonstrated on a xy feed table during circular tracking test. The friction compensation performances is analysed and compared for the following different control configurations:

(a) no friction feedforward and no inverse model disturbance observer
(b) static friction model feedforward
(c) GMS friction model feedforward
(d) inverse model disturbance observer
(e) static friction model feedforward and inverse model disturbance observer
(f) GMS model feedforward and inverse model disturbance observer

Figure 8 shows the circular test results of the various friction compensation schemes. Feedforward friction compensation and inverse model-based disturbance observer reduce the quadrant glitches considerably.

A combined disturbance observer and feedforward of GMS friction model yields the best quadrant glitch reduction. A quadrant glitch magnitude of less than 3 micrometer was recorded. Table 2 summarizes the experimental results.

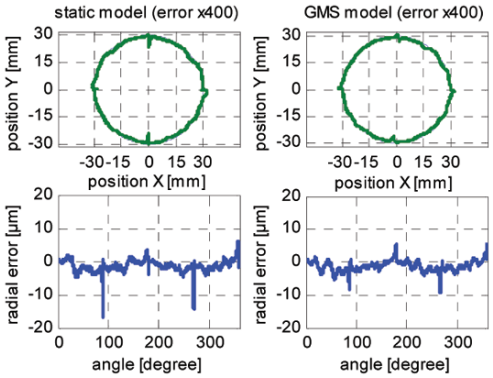

Fig. 9 Measured circular tests for tangential tracking velocity of 10 mm/s.

The improvement obtained by the GMS friction model over static friction model is small such that for this tangential tracking velocity (100 mm/s), the use of complex GMS friction model cannot be motivated. However, by reducing the tracking velocity to 10 mm/s, the presliding regime becomes more dominant and the benefit of using the GMS friction model that includes hysteresis with non local memory becomes more pronounced. This is illustrated in Figure 9.

5 Conclusions

Quadrant glitches, caused by the complex non-linear behaviour of friction at velocity reversal, can be compensated effectively using a combination of friction model feedforward and an inverse-model based disturbance observer. The benefits of using an advanced friction model like the Generalized Maxwell-slip (GMS) model are especially clear at slow motions where the pre-sliding friction is dominant. A simple approach based on separate pre-sliding and sliding measurements is presented to identify this complex GMS model.

Acknowledgements This work is supported by the Ministry of Higher Education, Malaysia and the Technical University Malaysia-Malacca. This work has been carried out within the framework of research project G.0446.06 of the Research Foundation – Flanders and also benefits from K.U.Leuven-BOF EF/05/006 Centre-of-Excellence Optimization in Engineering and from the Belgian Program on Interuniversity Poles of Attraction IAP VI/4 DYSCO (Dynamic Systems, Control and Optimization) initiated by the Belgian State, Prime Minister's Office for Science, Technology and Culture.

References

1. Al Bender, F., Lampaert, V., Swevers, J.: The Generalized Maxwell-Slip Friction Model: A Novel Model for Friction Simulation and Compensation. *IEEE Trans. on Automatic Control* **50**(11), 1883–1887 (2005).
2. Armstrong-Hélouvry, B.P., Dupont, Canudas de Wit, C.: A Survey of Models, Analysis Tools, and Compensation Methods for the Control of Machine with Frictions. *Automatica* **30**(7), 1083–1138 (1994).
3. Canudas de Wit, C. and Lishinsky, P.: Adaptive Friction Compensation with Partially Known Dynamic Friction Model. *Int. J. Adaptive Control and Signal Proc.* **11**, 65–80 (1997).
4. Dahl, P.R.: Measurement of Solid Friction Parameters of Ball Bearings. In *Proc. of 6th Annual Symp. on Incremental Motion, Control System and Devices* (1977).
5. Jamaludin, Z., Van Brussel, H., Swevers, J.: Classical Cascade and Sliding Mode Control Tracking Performances for a x-y Feed Table of a High-Speed Machine Tools. *Int. J. Precision Technology* **1**(1), 65–74 (2007).
6. Lampaert, V., Swevers, J., Al Bender, F., Ganseman, C., Prajogo, T.: Modification of the Leuven Integrated Friction Model Structure. *IEEE Trans. on Automatic Control* **47**(4), 683–687 (2002).
7. Tjahjowidodo, T., Al Bender, F., Van Brussel, H., Symens, W.: Friction Characterization and Compensation In Electro-Mechanical Systems. *J. of Sound and Vibration* **308**(3–5), 632–646 (2007).
8. Tung, E.D., Anwar, G., Tomizuka, M.: Low-Velocity Friction Compensation and Feedforward Solution Based on Repetitive Control. *J. Dynamics System Measurement and Control* **115**, 279–284 (1993).
9. Yi, L., Tomizuka, M.: Two-Degree-of-Freedom Control with Robust Feedback Control for Hard Disk Servo System. *IEEE/ASME Trans. on Mechatronics* **4**(1), 17–24 (1999).